FPGA-Based 2-D FIR Frost Beamformers with Digital Mutual Coupling Compensation

Sravan Pulipati[#1], Viduneth Ariyarathna[#], Ashira L. Jayaweera[$], Chamira U. S. Edussooriya[$2], Chamith Wijenayake[*3], Leonid Belostotski[^4], Arjuna Madanayake[#]

[#]Department Electrical and Computer Engineering, Florida International University, USA
[$]Department of Electronic and Telecommunication Engineering, University of Moratuwa, Sri Lanka
[*]School of Information Technology and Electrical Engineering, University of Queensland, Australia
[^]Department of Electrical and Computer Engineering, University of Calgary, Canada
[1]spuli009@fiu.edu, [2]chamira@uom.lk, [3]c.wijenayake@uq.edu.au, [4]lbelosto@ucalgary.ca

***Abstract*— This paper describes a technique for de-embedding electromagnetic mutual coupling effects between nearest neighbors of a ULA receiver. Measured S-parameters across a range of frequencies of interest are used in a closed-form mathematical model that relates measured S-parameters, measured LNA reflection coefficients, and transmission line parameters to digital beamformer design equations, such that the beam shape distortions arising from mutual coupling can be compensated in the DSP algorithm. A 5.8 GHz 32-element receiver array with custom receivers and 32-channel Xilinx Virtex-6 Sx35 FPGA based DSP system implementing a real-time complex-valued Frost beamformer operating at IF is proposed to show the benefits of de-embedding mutual coupling for far-field side-lobe suppression. The worst-case side-lobe level is reduced by 11.2 dB, and the average side-lobe level is reduced by 5.2 dB, for a 20 MHz IF signal.**

***Keywords*— RF beamforming, antenna arrays, mutual coupling, FIR filters, array signal processing.**

I. Introduction

Fully-digital beamforming is prevalent in a variety of radio-frequency (RF) antenna array systems, including phased-array radar, communications, space systems, positioning, and imaging [1]. Although a plethora of array factors can be realized with maximum flexibility and reconfigurability using fully-digital approaches, the real-time performance on an array of antenna elements is typically reduced due to non-ideal effects present in real-world antenna systems. In particular, the electromagnetic mutual coupling (MC) between neighboring elements and impedance mismatches between the antennas and the low-noise amplifiers (LNAs) across the radio band of interest causes significant deviation of the measured performance compared to theoretical best-cases developed in computer based simulations. For high-performance receiver arrays, the MC can significantly impact the stop-band performance (that is, the side-lobe (SL) level) of the receiver.

In this paper, we propose a wideband finite-impulse response (FIR) filter-based digital beamformer design that de-embeds the effect of MC from the array factor leading to improved SL performance. MC arises due to near field interaction of electric and magnetic fields which causes changes to element radiation patterns compared to the patterns of individual antennas [3], [4]. The MC depends on the antenna design, the array geometry and the inter-element spacing. Electromagnetic fields attenuate with distance from an antenna. Therefore, MC is dominant across its nearest neighbors in the array [4]. Measured MC using scattering (S-) parameters confirm it is negligibly small for arrays when the distance between antennas increases above a wavelength. Thus, we consider a low-order MC where each element couples to four nearest neighbors.

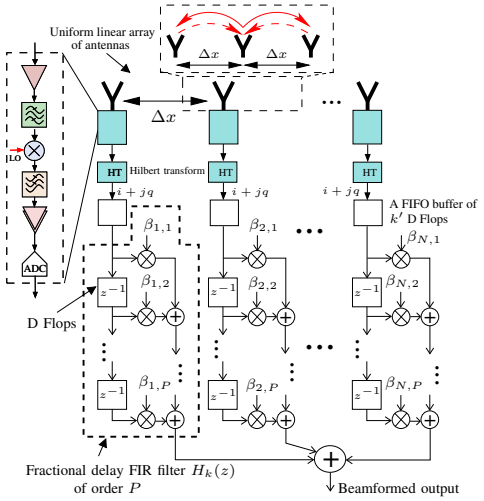

Fig. 1. Structure of a Frost beamformer [2]. The coefficients $\beta_{i,j}$ can be derived to realize either a true-time-delay beamformer or a more genetic 2-D FIR trapezoidal filter, while taking into account the effect of MC such that the effect of MC is de-embedded in the resulting overall array pattern.

In low-noise receivers, the LNA optimum reflection coefficient for minimum noise, Γ_{opt}, is designed to equal the array active reflection coefficient, Γ_{act}, for lowest noise [5]. Γ_{act} is beamformer dependent (i.e., beam-direction dependent) and differs from an isolated antenna-element reflection coefficient because of MC [5]. The underlining reason for beam-direction dependence has to do with the coupling of a noise wave emanating from LNA inputs to neighboring antennas where it is scaled by the beamformer before contributing to the output noise. When an LNA is connected to an isolated antenna, the antenna reflection coefficient can be designed such that the reflected portion of the noise emanating from the output destructively interferes

with the noise emanating from the output reducing the overall LNA noise at the system output to its theoretical minimum. In an array Γ_{act} is also calculated to maximize the cancellation of the correlated portion of the coupled noise and the noise emanating from the LNA output. However, the beam-direction dependent Γ_{act} makes such cancellation also beam-direction dependent. In addition, MC makes it impossible for LNA designers to simultaneously achieve input power match and noise match for all beam directions, thereby making array sensitivity beam dependent. Recent works [5] have used a Monte Carlo approach to finding Γ_{act} and LNA input reflection coefficient S_{11} that on average maximize sensitivity of an array. As was shown, the optimum S_{11} was rather high potentially causing stability problems and ripples in the LNA gain. To reduce the effects of MC on array noise, low scattering antennas were used in the array described in [6]. While this approach somewhat reduces design complexity, uncoupling antennas in the array would remove beam-dependence of Γ_{act} and would make LNA design similar to a more common single-antenna scenario.

II. Structured Coupling Matrix

The effect of electromagnetic MC can be modeled via a coupling matrix, whose elements are either estimated using numerous parametric estimation methods [7] or explicitly found, using methods such as Fourier decomposition of measured element patterns [8], measured using Wheeler caps [9] or measured S-parameter based formulations [10]. We employ S-parameter based approach, where a vector network analyzer is employed to obtain measurements of the S-parameters between nearest neighboring elements on the array. The measured S-parameters are not directly related to beamformer behavior due to the effects of the reflection coefficient at each LNA input port, and the finite propagation delay and transmission-line effects due to the finite length transmission lines that appear between antenna ports and their corresponding LNAs. The S-parameters lead to a coupling matrix $\mathbf{K}_c$, an $(N \times N)$ square matrix, for an N-element uniform linear array (ULA). This coupling matrix can be computed in terms of the S-parameters, transmission line characteristic impedance, and LNA driving point impedance, across each antenna location in the array. Following [10, Sec. II-A], the coupling matrix becomes $\mathbf{K}_c = \mathbf{Z}_A \left(\mathbf{Z}_M + \mathbf{Z}_A\right)^{-1}$, where $\mathbf{Z}_A = Z_A \mathbf{I}_N$, $\mathbf{Z}_M = \left(\mathbf{I}_N - \mathbf{S}\right)^{-1} \left(\mathbf{I}_N + \mathbf{S}\right) \mathbf{Z}_0$, and $\mathbf{Z}_0 = Z_0 \mathbf{I}_N$, where $\mathbf{S}$ is the measured S-parameter matrix, $\mathbf{I}_N$ is the $(N \times N)$ identity matrix, Z_0 is the characteristic impedance of the transmission line connecting the antenna to the LNA and Z_A is the LNA input impedance.

III. Signal Processing Model

The Frost digital beamforming structure is a general purpose FIR filterbank that implements a filter-and-sum output between multiple receivers. The Frost structure is employed for true-time-delay wideband beamformers by employing fractional delay filters as the FIR filters. Alternatively, the Frost structure can be utilized for realizing other wideband beamforming algorithms, including adaptive beamformers (e.g., Applebaum filters), adaptive nulling filters including spatial notch filters, and 2-D trapezoidal filters [11], [12].

A. Frost 2-D FIR Filter

The Frost beamformer can be described in z-domain as $Y(z) = \sum_{k=0}^{N-1} X_k(z) H_k(z)$ where $H_k(z)$ are the FIR filter transfer functions, and $X_k(z) \in \mathbb{C}$ are the z-transforms of the outputs of the digital receivers at antenna array location k on a ULA of receivers. In true time delay beamforming, the filter design problem amounts to approximating a series of time delays $\tau_k = k\frac{\Delta x}{c}\sin\theta$ in the digital domain, where c, Δx and θ are the wave speed, inter-antenna spacing, and beam direction, respectively. This is usually achieved by expressing the time delays in the form $\tau_k = k'T_s + \tau_f(k)$ where $0 \leq \tau_f(k) < T_s$, $k' = \lfloor k \sin\theta \frac{\Delta x}{cT_s} \rfloor$ and where $T_s = 1/F_s$ is the temporal sampling period of the analog to digital converters clocked at frequency F_s at each antenna. The FIR filters of order P take the form $H_k(z) = \sum_{i=0}^{P-1} \beta_{k,i} z^{-i}$, where the coefficients are selected based on a fractional time delay interpolation scheme. The integer delays of k' sample duration is realized as first-in first-out (FIFO) buffers using clocked D-flops; see Fig. 1.

Digital 2-D FIR filters having trapezoidal passbands [11], [12] in the 2-D space-time frequency domain provide wideband squint-free beams. Such 2-D FIR filters can be implemented using the Frost structure shown Fig. 1. In the case of a 2-D FIR trapezoidal filter of order $(N-1)\times(P-1)$, $\beta_{i,j}$ represents the value of the impulse response $h(n_x, n_t)$ of the 2-D FIR filter at $(n_x, n_t) = (i, j)$, where $0 \leq n_x \leq (N-1)$ and $0 \leq n_t \leq (P-1)$. Note that $h(n_x, n_t) \in \mathbb{C}^2$. In this case, the 2-D transfer function of the filter is given by $H(z_x, z_t) = \sum_{n_x=0}^{N-1} \sum_{n_t=0}^{P-1} h(n_x, n_t) z^{-n_x} z^{-n_t}$.

B. Frequency-Dependent Array Factor

Considering the outputs $X_k(z)$ of the digital receivers at each antenna, the directional 2-D input of the ULA can be expressed as $X(\theta, \omega) = X_k(e^{j\omega}) e^{-jk\omega\sin\theta}$, where θ is the direction measured from array broadside and $\omega < 2\pi F_s/2$ is the normalized (radian) frequency. The array output in the 2-D angular-frequency domain is therefore given by $Y(\theta, \omega) = X(\theta, \omega) H_T(\theta, \omega)$, where $H_T(\theta, \omega)$ denotes the total array pattern of the directional receiver, which, following the principle of pattern multiplication is given by $H_T(\theta, \omega) = H_E(\theta, \omega) H_A(\theta, \omega) H_M(\theta, \omega)$, where $H_E(\theta, \omega)$ is the element radiation pattern of a signal antenna in isolation, $H_A(\theta, \omega)$ is the array factor produced by the Frost beamformer, and $H_M(\theta, \omega)$ represents (undesired) distortions in the array pattern caused by the effect of MC. Here, the array factor of the Frost beamformer is given by $H_A(\theta, \omega) = \sum_{k=0}^{N-1} H_k(e^{j\omega}) e^{-jk\omega\sin\theta} = \sum_{k=0}^{N-1} \sum_{m=0}^{P-1} \beta_{k,m} e^{-j\omega(m + k\sin\theta)}$, having the magnitude response $\rho(\theta, \omega) = \|H_A(\theta, \omega)\|$. Next, we design the Frost beamformer to produce $H_A(\theta, \omega)$ which can de-embed the effect of MC by explicitly considering the multiplicative coupling transfer function $H_M(\theta, \omega)$ during filter design.

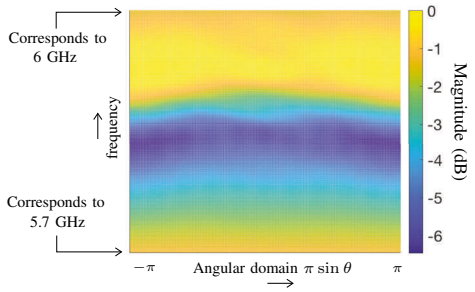

Fig. 2. Magnitude of the MC transfer function $H_M(\theta,\omega)$ computed using experimentally measured S-parameters of 6 nearest neighbors with $\eta = 4$.

C. Proposed Design with Compensation of MC

The MC produces a coupling transfer function $H_M(\theta,\omega)$ that is both angle and frequency dependent. The presence of MC modifies the input signal from the array such that if the original input signal is $X(\theta,\omega)$ the signal that is practically available at the output of the ULA is $X(\theta,\omega)H_M(\theta,\omega)$. The coupling function can be obtained by the structured coupling matrix $\mathbf{K}_c = [K_{m,n}]_{N\times N}$ containing frequency dependent elements, mentioned above in Section II as $H_M(\theta,\omega) = K_{\eta,\eta}(\omega) + \sum_{n=1}^{\eta-1}\left(K_{\eta,\eta-n}(\omega)e^{j\omega n\sin\theta} + K_{\eta,\eta+n}(\omega)e^{-j\omega n\sin\theta}\right)$, where the index η defines the model order of the MC function [10]. For this work, we selected $\eta = 4$, leading to coupling from six nearest neighboring elements in the ULA. Fig. 2 shows the magnitude of the coupling function for our ULA setup, computed using measured S-parameters. This coupling function modifies the beamformer array factor to $H_A(\theta,\omega)H_M(\theta,\omega)$. Therefore, we propose that the FIR filters in the beamformer be modified using an MC compensation function $\frac{1}{\|H_M(\theta,\omega)\|+\epsilon}$, where $\epsilon > 0$ is a small real-valued constant chosen to avoid division by zero at the zeros of $H_M(\theta,\omega)$ yielding the required form $\rho_{new}(\theta,\omega) = \|H_M(\theta,\omega)\| \cdot \left\|\sum_{k=0}^{N-1} \frac{H_k(e^{j\omega})e^{-j\omega k\sin\theta}}{\|H_M(\theta,\omega)\|+\epsilon}\right\| \approx \rho(\theta,\omega)$. Small ϵ limits the depth of array factor nulls to $-10\log_{10}\epsilon^2$. Typical values around $\epsilon = 0.01$ leads to nulls that do not go down below -40 dB after compensation of MC.

IV. Antenna Array Design

We present the design of the antennas array, RF frond-end and the beamformer in this section. We employ a 2-D FIR trapezoidal filter as the beamformer. The antenna array and the RF front-end is described in the next subsection.

A. Array, RF Front-End and Receivers

The antenna array consists of 32-element ULA where each element is a 4-element vertical subarray that provides an enhanced gain in the elevation pattern. The horizontal spacing of the antenna array has been set to 31 mm. As shown in Fig. 1, the front-end includes a single mixer-based receiver architecture. The receiver chain includes a LNA (16 dB gain at 5.8 GHz, 2.4 dB noise figure), bandpass filter, mixer, lowpass filter, and an intermediate-frequency (IF) amplifier ($\approx$ 30 dB gain). All 32 IF channels are sampled in the ROACH-2 platform using 2 ADC16x250-8 analog-to-digital converter

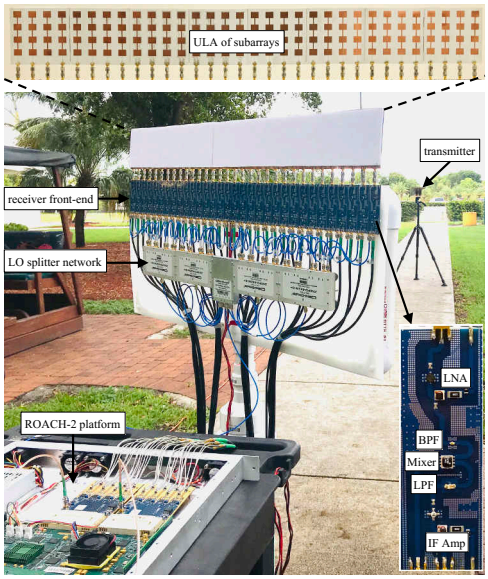

Fig. 3. The 5.8 GHz 32-element antenna array setup used for experimentally verifying the proposed approach.

(ADC) cards, where each card supports 16 analog channels at a rate of 240 MSps. An FIR filter based implementation of the Hilber transform is used to obtain the in-phase and quadrature-phase (IQ) channels for each sampled IF channel. The IQ digital streams of each channel are then used for calibrating each receiver channel to get rid of gain and phase mismatches by using a complex multiplier in the data path.

B. Design of 2-D FIR Trapezoidal Filter

In the proposed MC-compensated beamformer, a 2-D FIR trapezoidal filter having a linear phase response and approximately equal SL levels is employed. The 2-D FIR trapezoidal filter design is formulated as a convex optimization problem [13]. In order to achieve approximately equal SL levels, the optimal design, i.e., the impulse response $h(n_x,n_{ct})$, is obtained with respect to ℓ_∞ norm (called the minimax design). This convex optimization problem can be converted to a second-order cone programing problem, which can be efficiently solved using optimization toolboxes with MATLAB. Due to the limited space, the problem formulation is not presented here, and the reader is referred to [14] for a formulation of minimax design of 2-D FIR filters, however, with real-valued impulse responses.

V. Experimental Validation

A. 2-D FIR Trapezoidal Filter on Frost Structure

The 2-D FIR trapezoidal filter is realized at a bandwidth of $\pm$30 MHz centered at 5.860 GHz. The number of antennas and dedicated receivers (i.e., N) is 32, see Fig. 3. 2-D FIR trapezoidal filters with and without the proposed MC compensation are implemented and tested in real-time to evaluate the relative improvements of SL levels (i.e., directional beam selectivity as a function of frequency across the 30 MHz band of interest). Fig. 4 shows measured beam patterns obtained for three different IFs where the center

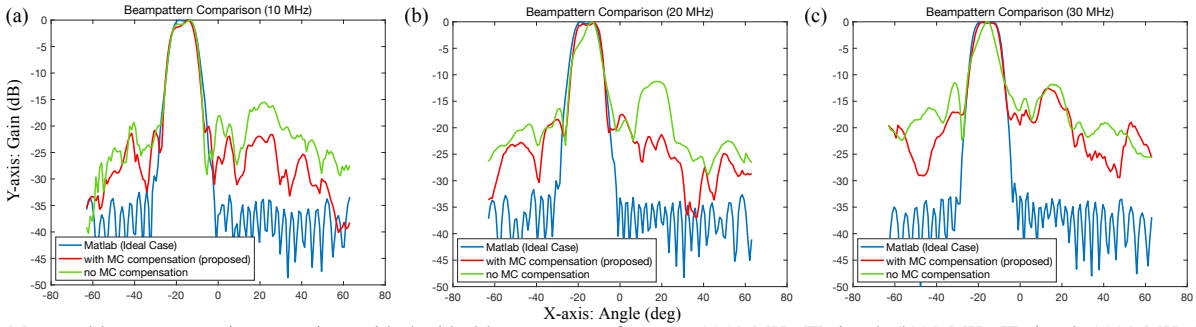

Fig. 4. Measured beam patterns in comparison with the ideal beam patterns for cases (a)10 MHz IF signal; (b)20 MHz IF signal; (c)30 MHz IF signal.

Table 1. SL Level Reductions Achieved with the Proposed Approach

Parameter (dB)	IF		
	10 MHz	20 MHz	30 MHz
Reduction of worst-case SL level	7.5	11.2	5.6
Reduction of average SL level	5.1	5.2	2.1
Maximum reduction of SL level	12.1	13.5	11.7

frequency was fixed at 5.8 GHz. The IFs were selected at 10 MHz, 20 MHz, and 30 MHz, with a digital clock frequency (same as ADC sample frequency) of 160 MHz. The transmitter was a horn antenna (gain 13 dBi) placed in the array plane at a distance of 6.3 m.

B. Experimental Errors

The presence of 32 elements requires a relatively large area for experiments because the near field region now extends to about 700λ. The use of a fully anechoic antenna test chamber of such dimensions is prohibitively expensive for the authors; therefore, a large underground parking garage was used for conducting the experiments. The garage was clear of obstacles within 4 m height but there exists metal piping close to the ceiling which causes some strong reflections. The concrete ceiling and tarred floor of the building are also expected to contribute to strong multipath reflections which prevents more accurate measurement of SLs and directional nulls.

C. Discussion

The paper describes real-time antenna, microwave and digital signal processing systems for implementing digital Frost beamforming receivers across up to 32 antenna elements on a ULA. The 5.8 GHz realization supports up to 100 MHz of bandwidth but non-ideal effects in the antenna array and microwave circuitry limits performance compared to theoretical best-case of the digital beamformers. The reflections in the measurement chamber further degrades measurement of the deep SLs. However, we demonstrate that measured S-parameters from the antenna array can lead to optimized digital circuit designs that de-embed the MC effects between elements up to the first order, thereby allowing reduced SLs compared to direct implementation of a given digital beamformer. The improvements in SL performance by the proposed approach is shown in Table 1 for the 30 MHz band. We observe 5.2 dB and 13.5 dB reductions in the average SL level and the worst-case SL level, respectively, at an IF of 20 MHz. Furthermore, more than 11.7 dB maximum reduction of SL levels are achieved for the 30 MHz band.

VI. Conclusions

Side-lobes of Frost beamformers are improved when measured MC between elements obtained from S-parameters are de-embedded in the digital domain during beamformer design. Experimental results confirm that > 5 dB (average) SL level reduction can be achieved with the proposed MC de-embedding with a 2-D FIR Frost beamformer having 20 MHz bandwidth.

Acknowledgment

Authors thank NSF ECCS 1711625 and the University of Moratuwa for financial support.

References

[1] S. H. Talisa *et al.*, "Benefits of digital phased array radars," *Proc. of the IEEE*, vol. 104, no. 3, pp. 530–543, Mar. 2016.
[2] Harry L. Van Trees, *Optimum Array Processing: Part IV of Detection, Estimation, and Modulation Theory*. NY: John Wiley & Sons, 2002.
[3] Z. Zheng *et al.*, "MISC array: A new sparse array design achieving increased degrees of freedom and reduced mutual coupling effect," *IEEE Trans. on Signal Processing*, vol. 67, no. 7, pp. 1728–1741, Apr. 2019.
[4] ——, "Robust adaptive beamforming against mutual coupling based on mutual coupling coefficients estimation," *IEEE Trans. on Vehicular Technology*, vol. 66, no. 10, pp. 9124–9133, Oct. 2017.
[5] L. Belostotski *et al.*, "Low-noise amplifier design considerations for use in antenna arrays," *IEEE Trans. on Antennas and Propagation*, vol. 63, no. 6, pp. 2508–2520, Jun. 2015.
[6] D. Jones et. al., "Modeled and measured mutual impedances, element patterns, and sensitivity for a 19 element focal plane array," in *Proc. IEEE Antennas and Propagation Society International Symposium*, 2008, pp. 1–4.
[7] T. Svantesson, "Mutual coupling compensation using subspace fitting," in *Proc. IEEE Sensor Array and Multichannel Signal Processing Workshop*, 2000, pp. 494–498.
[8] H. Steyskal and J. S. Herd, "Mutual coupling compensation in small array antennas," *IEEE Transactions on Antennas and Propagation*, vol. 38, no. 12, pp. 1971–1975, Dec. 1990.
[9] S. De Silva *et al.*, "Modeling and measuring of antenna array S-parameters and radiation efficiency," in *IEEE International Symposium on Antennas and Propagation*, 2017, pp. 2293–2294.
[10] J. Kota *et al.*, "A 2-D signal processing model to predict the effect of mutual coupling on array factor," *IEEE Antennas and Wireless Propagation Letters*, vol. 12, pp. 1264–1267, 2013.
[11] T. K. Gunaratne and L. T. Bruton, "Broadband beamforming of bandpass plane waves using 2D FIR trapezoidal filters at baseband," in *Proc. IEEE Asia Pacific Conf. Circuits Syst.*, Dec. 2006, pp. 546–549.
[12] ——, "Beamforming of broad-band bandpass plane waves using polyphase 2-D FIR trapezoidal filters," *IEEE Trans. on Circuits Syst.*, vol. 55, no. 3, pp. 838–850, Apr. 2008.
[13] A. Antoniou and W.-S. Lu, *Practical Optimization: Algorithms and Engineering Applications*. NY: Springer, 2007.
[14] W.-S. Lu and T. Hinamoto, "A second-order cone programming approach for minimax design of 2-D FIR filters with low group delay," in *Proc. IEEE Int. Symp. Circuits Syst.*, 2006, pp. 2521–2524.